TECHNISCHE
UNIVERSITÄT
DARMSTADT

INSTITUT FÜR KERNPHYSIK

A. RICHTER

RECENT RESULTS ON THE MAGNETIC DIPOLE AND QUADRUPOLE RESPONSE IN NUCLEI PROBED IN ELECTRON AND PHOTON SCATTERING

Invited talk presented at the International Symposium
New Facet of Spin Giant Resonances in Nuclei,
November 17–20, 1997,
Graduate School of Science, University of Tokyo, Tokyo, Japan

January 1998

IKDA 98/03

RECENT RESULTS ON THE MAGNETIC DIPOLE AND QUADRUPOLE RESPONSE IN NUCLEI PROBED IN ELECTRON AND PHOTON SCATTERING

A. RICHTER
Technische Universität Darmstadt,
Schlossgartenstr. 9, D–64289 Darmstadt, Germany
E-mail: richter@ikp.tu-darmstadt.de

Results on ongoing research of elementary magnetic nuclear excitations using photon and electron scattering at the superconducting Darmstadt electron linear accelerator (S-DALINAC) are presented. In the first part of the talk properties of the orbital magnetic dipole scissors mode are discussed which has now been studied throughout the rare-earth nuclei including the transitional regions from spherical vibrators to rotors and from rotors to nuclei with γ-soft shapes. The associated strong variations of the total $B(\mathrm{M1})$ strength and their correlation with the $B(\mathrm{E2})$ transitions to the 2_1^+ states, which define the degree of deformation, have recently been successfully explained by a phenomenological approach as well as by the Interacting Boson Model. High-quality (γ,γ') spectroscopy with a EUROBALL cluster module in combination with a statistical analysis of unresolved background contributions demonstrates that contrary to claims of a severe reduction, the scissors mode strength in odd-mass nuclei is comparable to that in the even-even neighbours. The second part of the talk is concerned with high-resolution inelastic electron scattering at 180°, which is selective with respect to magnetic excitations. As a first example the investigation of an ℓ-forbidden M1 transition from the ground state to the $J^\pi = 1^+$ state at $E_x = 7.003$ MeV in ^{32}S is discussed. The extracted $B(\mathrm{M1})$ strength of 0.0035 μ_N^2 is the smallest ever measured with electron scattering and constitutes one of the most sensitive tests of the role of non-nuclear degrees of freedom in the nuclear magnetic response. Finally, systematic studies on the hitherto scarcely explored magnetic quadrupole giant resonance which is mainly a spin-isospin excitation located at an excitation energy $E_x \approx 44 \cdot A^{-1/3}$ MeV are discussed. In the last experiments a dramatic improvement of the background reduction was achieved by the use of the pulsed beam structure originally developed for the Free Electron Laser at the S-DALINAC. This allows access to heavy nuclei for the first time. Results for the strongly fragmented and quenched M2 strength are presented for ^{48}Ca and ^{90}Zr and compared to SRPA calculations and sum rule approaches. Finally, possible implications of these results with respect to certain questions in astrophysics and in-medium vector meson mass scaling (Brown-Rho scaling) are also mentioned.

1 Introduction

This symposium on "New Facet of Spin Giant Resonances in Nuclei" deals with topics which would have been much to the heart and interest of Franz Osterfeld. His untimely death prevents him to be with us as originally planned. Speaking about spin-isospin excitations I cannot help thinking of his many important

contributions to this field and I thus dedicate this talk to the memory of Franz, a fine physicist and a good friend.

The talk is composed of two parts. Firstly, I will remark – along the lines of previous talks – on the nature and our present knowledge of the orbital and spin magnetic dipole response in heavy deformed even and odd mass nuclei. Secondly, inelastic electron scattering at 180° is considered and three particular examples of recent experiments performed at the S-DALINAC [1] are outlined: the measurement of an ℓ-forbidden magnetic dipole transition in ^{32}S, the determination of the magnetic quadrupole response in ^{48}Ca and likewise the one in ^{90}Zr. The new experimental data are discussed in the light of extensive theoretical model predictions and of sum rules. Considering the wealth of material presented in the actual talk the rather limited space allowed for its written version in these proceedings forces me to restrict myself essentially only to a summary of the various topics I did present and discuss orally. For the same reason, the list of references given at the end will not be complete and I thus focus the attention of the reader to the many additional references given in the articles cited and the articles to appear soon on our new results from the inelastic electron scattering experiments at 180°.

2 Orbital and spin magnetic dipole response in heavy deformed nuclei

2.1 Overview

Magnetic dipole excitations in heavy deformed nuclei constitute a field of intensive experimental and theoretical research over the last decade [2–5]. The interest has been triggered by the discovery [6] of an elementary orbital magnetic dipole mode at low excitation energies – the so-called scissors mode. Subsequently, it was also possible to experimentally pin down the existence of a giant spin M1 resonance at somewhat higher excitation energies in rare-earth and actinide nuclei [7,8]. A rather consistent picture of the magnetic dipole response in heavy deformed nuclei is emerging from the experimental information gathered over the last years. It is presented here by way of example in Fig. 1 for the case of the nucleus ^{154}Sm.

The scissors mode is located at excitation energies between 2 and 4 MeV, and its strength is typically fragmented into about 10 transitions. Its total strength is proportional to the square of the ground state deformation [9] and saturates [10] in well deformed nuclei (with roughly constant deformation) at a value $B(\mathrm{M1})\uparrow \approx 3\mu_N^2$. The almost pure orbital character of the M1 transitions was demonstrated by the comparison of electron and photon scattering, which include the coherent contributions of spin and orbital matrix elements, with

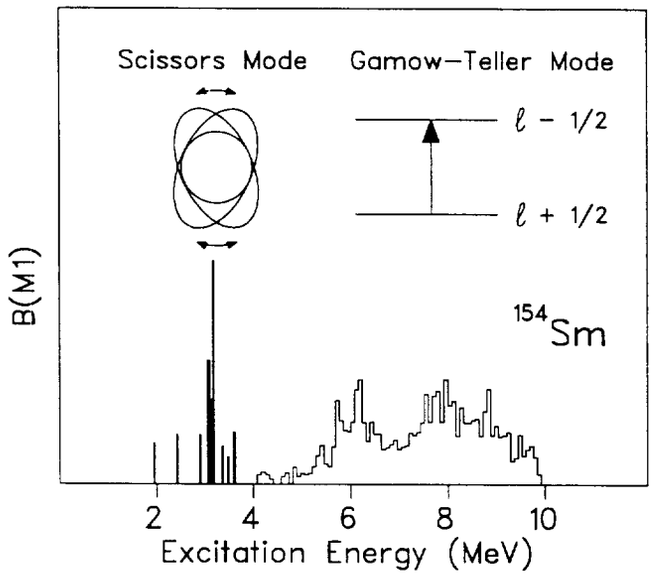

Figure 1: M1 response in a heavy deformed nucleus.

inelastic proton scattering, which is sensitive only to the spin-isospin part of the nucleon-nucleon interaction [11]. The latter probe, however, revealed the existence of a giant spin-flip M1 resonance at higher excitation energies [7,8]. It is located in the energy region $E_x \approx 5 - 10$ MeV and exhibits a characteristic double hump structure whose origin is still subject of controverse interpretations [3]. Its strength is $B(\mathrm{M1})\uparrow \approx 11\mu_N^2$, almost constant throughout the rare-earth region and approximately independent of deformation [3]. There are hints of considerable fine structure of the resonance observed in a high-resolution photon scattering experiment [12] on ^{154}Sm which also indicates that destructive interference effects of orbital admixtures to the spin strength might be present.

2.2 Sum rules for the scissors mode

With the large body of data collected it becomes feasible to study the properties of the scissors mode systematically in rare-earth nuclei [3,13]. A central topic is the question whether the characteristic strength variation can be understood in terms of fundamental quantities such as sum rules for the magnetic transition strength [14]. Two approaches are discussed here. The first is based

on a phenomenological expression [15] which was derived within the two-rotor model [16] but is valid in a general context of the following sum rule

$$B(\mathrm{M1})\uparrow \simeq \frac{3}{16\pi}\,\Theta_{sc}\,E_{sc}\,(g_p-g_n)^2\,\mu_N^2\,. \qquad (1)$$

Here, E_{sc} denotes the energy of the mode, and Θ_{sc} represents the mass parameter very close to the moment of inertia which can be estimated from the "classical" sum rule for E2 strength derived by Bohr and Mottelson [17]. One arrives at a simple expression

$$B(\mathrm{M1})\uparrow \simeq \left\{0.0042\,\frac{4NZ}{A^2}\,E_{sc}\,A^{5/3}\,\delta^2\,(g_p-g_n)^2\right\}\mu_N^2\,, \qquad (2)$$

which also contains explicitly the experimentally found dependence of the M1 strength on the square of the g.s. deformation parameter δ.

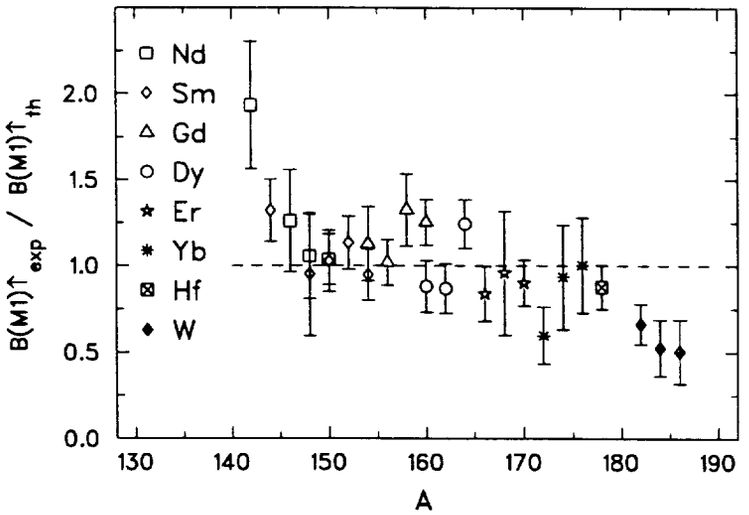

Figure 2: Ratio of the experimental $B(\mathrm{M1})$ strength and the phenomenological sum rule [15] prediction for the scissors mode strength plotted as a function of the mass number. The $B(\mathrm{M1})$ sum rule strength is exhausted by most nuclei.

Figure 2 displays the ratio of experimental $B(\mathrm{M1})$ strength and the prediction of Eq. (1) assuming a constant value of E_x of 3 MeV and gyromagnetic factors $g_p = 2Z/A$ and $g_n = 0$. One finds a very satisfactory description of the strength for most nuclei confirming the deformation dependence. Some deviations are observed corresponding to transitional regions from vibrators

to rotors ($A \simeq 140 - 150$) and from rotors to γ-soft nuclei ($A \simeq 180 - 190$). The good quantitative reproduction also indicates that the complete strength is detected in the experiments.

Recently, also a description within the IBM-2 could be achieved [18]. It starts from a sum-rule derived by Ginocchio [19]

$$\sum_f B(\mathrm{M1}: 0^+ \rightarrow 1_f^+)\uparrow \; = \; \frac{9}{4\pi}(g_\pi - g_\nu)^2 \frac{P}{N-1}\langle 0|N_d|0\rangle \qquad (3)$$

with N being the total number of bosons, and $P = N_\pi N_\nu/(N_\pi + N_\nu)$. Equation (3) relates the scissors mode strength to the average number of quadrupole bosons in the g.s., $\bar{N}_d = \langle 0|N_d|0\rangle/N$, which can be expressed by a deformation parameter β. A relation was derived [18] between this IBM-specific quantity and geometrical definitions of deformation like the Bohr-Mottelson parameter β_2

$$\beta \; = \; \frac{\lambda}{\frac{2}{3}\sqrt{\pi}} \left(\frac{Z}{Z_{\mathrm{val}}}\right) \beta_2 \, . \qquad (4)$$

Here, Z_{val} describes the number of protons in the valence shell, and λ is a measure of the exhaustion of the E2 sum rule by the transition to the 2_1^+ state. Figure 3 compares the resulting predictions of the B(M1) strength to the experimental findings as a function of the total boson number N. Clearly, a very satisfactory description of the data over a wide mass range (Nd to W) is achieved.

Overall, one can conclude that the systematics of the scissors mode strength in rare-earth nuclei with even mass numbers is well understood now, and the approaches presented here are likely to provide a description of the actinide region as well. What remains open are extensions of the models to the regions of γ-soft nuclei ($A \approx 130$ and $A \approx 190$), where first experimental observations of the scissors mode were recently reported [20,21].

2.3 Dipole strength in odd-mass nuclei

For a number of reasons a search for the scissors mode in odd-mass nuclei is considerably more complicated. Because of the high level densities fragmentation of the mode should be enhanced, and experimentally – unlike in the case of even-mass nuclei – no parity information can be derived from the photon scattering experiments. It is well known from the investigations in the even-mass cases that non-negligible E1 strength is found in the energy interval over which the scissors mode is spread and that it varies considerably for different nuclei [22].

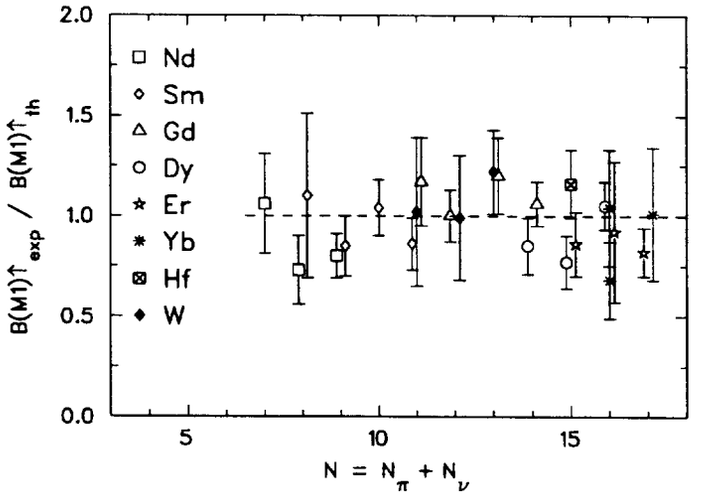

Figure 3: Ratio of the experimental $B(\mathrm{M1})$ strength and the IBM-2 sum rule prediction for the scissors mode strength plotted as a function of the boson number. The IBM-2 sum rule provides a systematic description of all experimental data from Nd to W.

The experimental information gained so far from (γ, γ') experiments for odd-mass cases [23–27] is summarized in Fig. 4. In the upper part, the dipole strength distributions are shown. (Note that the strength is given by the quantity $g\Gamma_0^{\mathrm{red}} = \Gamma_0/E_x^3$ proportional to $B(\mathrm{E1})$ and $B(\mathrm{M1})$ because of the experimental indistinguishability.) Dramatic variations are observed for the number of transitions, the average dipole strength and the distribution over the energy interval which are impossible to understand by simple coupling pictures of the unpaired nucleon. The problems are further aggravated when considering the total strength of the mode seen in the experiments. Assuming as an extreme upper limit that all observed g.s. transitions have M1 character, the summed $B(\mathrm{M1})$ values are depicted in the lower part of Fig. 4. Reduction factors of $2-3$ compared to the average value of about 3 μ_N^2 in well deformed nuclei are found in clear contradiction to all theoretical predictions (see Refs. [28,29] as examples).

A solution of this puzzling situation has been presented very recently [30]. Because of the high level densities in the investigated nuclei the strength is very fragmented and furthermore even the high resolution of Ge detectors is no longer sufficient to resolve the individual transitions. However, the part of the dipole strength hidden in the background of the spectra can be extracted by means of a fluctuation analysis based on a statistical treatment, i.e. assum-

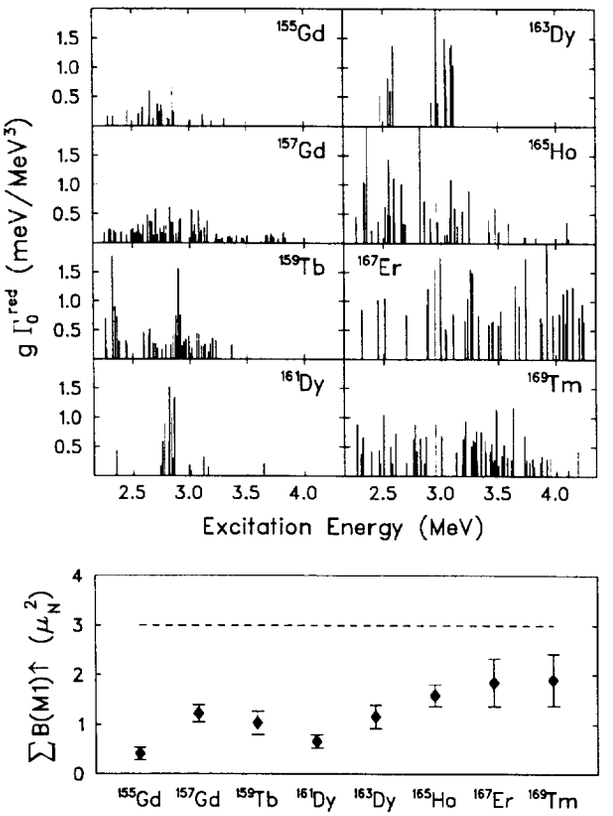

Figure 4: The comparison of the dipole strength in the odd-mass nuclei show large differences in total strength, fragmentation and the number of detected ground state transitions.

ing Wigner-type level spacing and Porter-Thomas intensity strength distributions[31]. Such an analysis was performed for the high-quality data measured for ^{165}Ho and ^{169}Tm at the S-DALINAC with a EUROBALL cluster module [27] providing evidence for significant contributions in the background. If these are included the strong reduction of the total B(M1) strengths disappears and values comparable to the even-mass neighbours are found. Subsequently, these findings have been confirmed using a set of data on the nucleus ^{157}Gd measured under completely different experimental conditions [32].

It can be shown [30] that the statistical assumptions underlying the fluctuation analysis approach are also capable to explain the large variations of the

measured dipole distributions in Fig. 4. Monte-Carlo distributions have been generated taking into account the properties of M1 and E1 distributions in the even-mass neighbors and allowing for the energy dependence of the experimental sensitivity limits. The results are compared to the experiments in Fig. 5

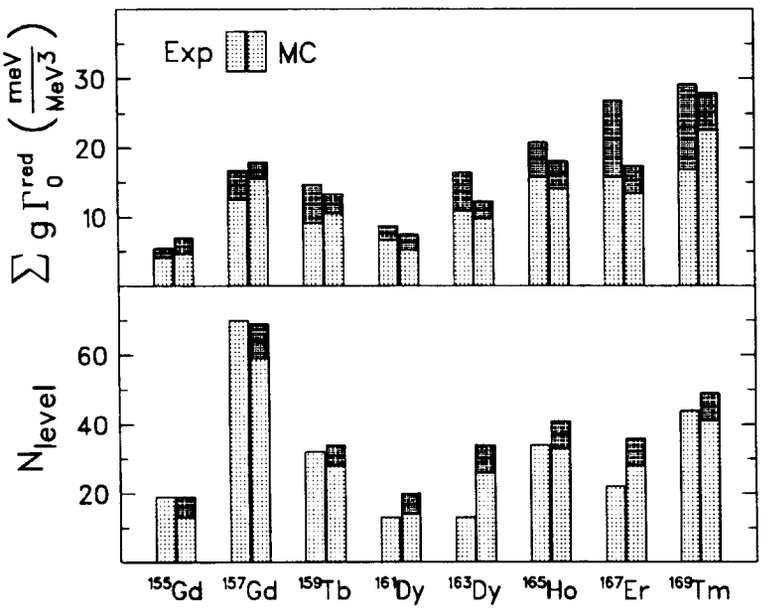

Figure 5: Reproduction of the experimental dipole strength and the number of ground state transitions (Exp) by Monte Carlo methods (MC).

for the summed dipole strength $\sum g\Gamma_0^{red}$ visible above the detection thresholds and for the total number of observed levels. Overall, the large variations of both quantites for the investigated nuclei can be simultaneously reproduced in a very satisfactory manner. Thus, one can conclude that the scissors mode strength is also present in odd-mass nuclei, but non-negligible (and varying) parts of it might escape direct detection in the photon scattering experiments.

3 Inelastic electron scattering at 180°

3.1 Experimental matters

Recently, a new system for high-resolution electron scattering at 180° has been installed[33] at the S-DALINAC. It is a particulary attractive experimental tool

for the study of magnetic transitions. At 180° the longitudinal part of the cross section essentially disappears while the transverse contribution remains finite. Magnetic transitions – which are of purely transverse character – are thus strongly enhanced at 180° where furthermore the elastic radiative tail is largely suppressed.

The present device shows a number of exceptional features[33] compared to previous 180° systems, firstly because of the coupling of the system to a large-aperture, large-momentum-acceptance QCLAM magnetic spectrometer[34] and secondly because of the fact that due to the suppression of instrumental background and an improved event reconstruction [35] very clean electron spectra can be obtained. In nuclear physics experiments at the S-DALINAC, for the first time the 10 MHz pulsed beam developed for using the linac as a driver for a Free Electron Laser[36] has been employed to single out the scattered electrons from the target, i.e. the true events from electrons resulting from slit or backscattering ending up in the focal plane detectors of the QCLAM spectrometer. The time of flight differences of the detected electrons allow a distinction between the true and false events and finally the signal to background ratio in the spectra could be increased by almost an order of magnitude.

The main properties of the 180° scattering system at the S-DALINAC can be summarized as follows:

- maximum central momentum 95 MeV/c
- momentum acceptance −6% to +8%
- horizontal and vertical opening angles ±40 mrad
- solid angle 6.4 msr
- intrinsic momentum resolution 2×10^{-4}

For comparison typical values of older 180° systems for horizontal acceptances and solid angles were ±15 mrad and 1 msr, respectively. The central momentum range of our system is sufficient for the observation of M1, M2 and M3 transitions and the maximum value of 95 MeV/c roughly corresponds to the first maximum of a M3 form factor.

In a first experiment the magnetic dipole and magnetic quadrupole response of ^{28}Si up to an excitation energy of $E_x \simeq 19$ MeV has been investigated [37–39] with the particular emphasis on determining the enhancement of isovector M1 strength due to meson exchange currents by comparing B(M1) and Gamow-Teller strength distributions in self-conjugate nuclei [40]. Rather than repeating the salient features of the experimental results and their theoretical interpretation which can be found in the references cited, I will next discuss three new and unpublished experiments bearing on certain aspects of the physics of spin-isospin excitations.

3.2 First example: an ℓ-forbidden magnetic dipole transition in ^{32}S

The magnetic dipole response serves as a unique testing area for the role of non-nuclear degrees of freedom in the nuclear dynamics. It is well established that the phenomenon of quenching of the B(M1) strength is partly due to the contributions by mesonic exchange currents (MEC) and Δ-hole excitations, although their quantitative role is still a subject of considerable debate.

The *sd*-shell mass region is a favorable ground for such investigations because of the possibility to perform full $0\hbar\omega$ shell-model calculations [41]. The experimentally observed quenching has been successfully described for *sd*-shell nuclei by the introduction of an effective operator and the necessary renormalization factors were determined either empirically [42] or analytically [43,44]. While the analytical results generally agree quite well with each other and also with the empirical results for the spin and orbital parts, a considerable discrepancy is found for the isovector tensor correction [42]. The investigation of ℓ-forbidden M1 transitions (which are of $1d_{3/2} \leftrightarrow 2s_{1/2}$ type in *sd*-shell nuclei) provides maybe the most promising approach to this problem because of the strong suppression of the usually dominating spin matrix element. The higher-order corrections to the ℓ-forbidden transitions are expected to be dominated by Δ admixtures into the nuclear wave functions [43,44] and it is a unique observable in this respect. When scaled to the free-nucleon strength, the Δ correction is expected to be essentially the same for the isovector $M1$ and GT operators [42]. However, an analysis of the ℓ-forbidden $1d_{3/2} \rightarrow 2s_{1/2}$ "single-hole" transitions in $A = 39$ nuclei gives an $M1$ strength relative to the GT strength which is about an order of magnitude larger than expected (see Ref. [45] and references therein). Indeed, this is one of the major problems remaining in our understanding of electromagnetic and β-decay observables in light nuclei.

One possibility of explaining this discrepancy is that the $A = 39$ transitions are not well described by pure $1d_{3/2}$ and $2s_{1/2}$ single-hole states, and that low-lying core excitations from the *sd*-shell across the fp-shell could introduce some allowed strength in a way which is not well understood. Therefore it is important to examine a case away from the end of the *sd*-shell, where such low-lying core excitations should be less important, in order to see if the discrepancy persists. The very weak M1 transition at $E_x = 7.003$ MeV in ^{32}S and the analog g.s. GT decays in ^{32}Cl and ^{32}P are perhaps the best example available for a study of ℓ-forbidden strength towards the middle of the *sd*-shell. Here, we present for the first time a B(M1) value for the extremely weak ℓ-forbidden transition in ^{32}S derived from electron scattering. This information is of particular interest for a combined analysis with the GT strengths to test the *sd*-shell wave functions and the effects of higher-order corrections.

The ^{32}S(e,e') reaction has been measured at the S-DALINAC with the 180° system described above. Additional unpublished data were available from previous experiments at the high-resolution energy-loss spectrometer. In total, a momentum transfer range $q_{eff} \simeq 0.3 - 0.9\,\mathrm{fm}^{-1}$ was covered. The transverse form factor of the transition to the 1^+ level at 7.003 MeV is depicted in Fig. 6. The comparison to a typical $1d_{5/2} \rightarrow 1d_{3/2}$ spin-flip form factor (dashed line)

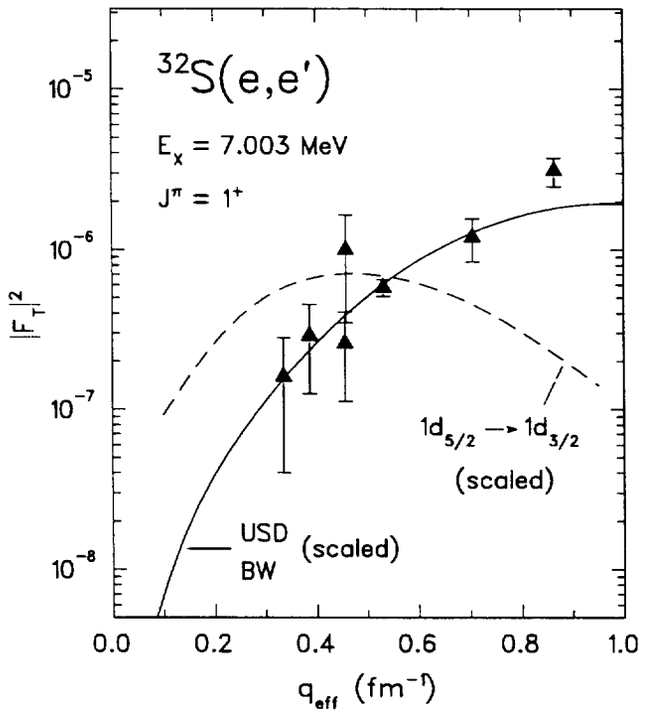

Figure 6: Form factor of the ℓ-forbidden M1 transition to the $J^\pi = 1^+$ state at $E_x = 7.003$ MeV in ^{32}S. The extracted B(M1) strength of 0.0035 μ_N^2 is obtained by extrapolation of the form factor to the photon point and constitutes the smallest ever measured with electron scattering.

reveals an anomalous dependence on the momentum transfer. However, this can be satisfactorily described by a shell-model calculation with the unified *sd*-shell (USD) interaction[41], but the calculation is based on free nucleon g-factors, because the q dependence of the higher-order corrections is not known. Thus, the absolute value must be scaled down by a factor of about four to describe the data. Nevertheless, the good description of the q dependence allows an

extrapolation to the photon point in order to extract the $B(\mathrm{M1})$ strength. One finds an extremely small number, $B(\mathrm{M1})\uparrow = 0.0035(4)\ \mu_N^2$, which, to the best of our knowledge, is the smallest value ever reported for an M1 transition in electron scattering experiments.

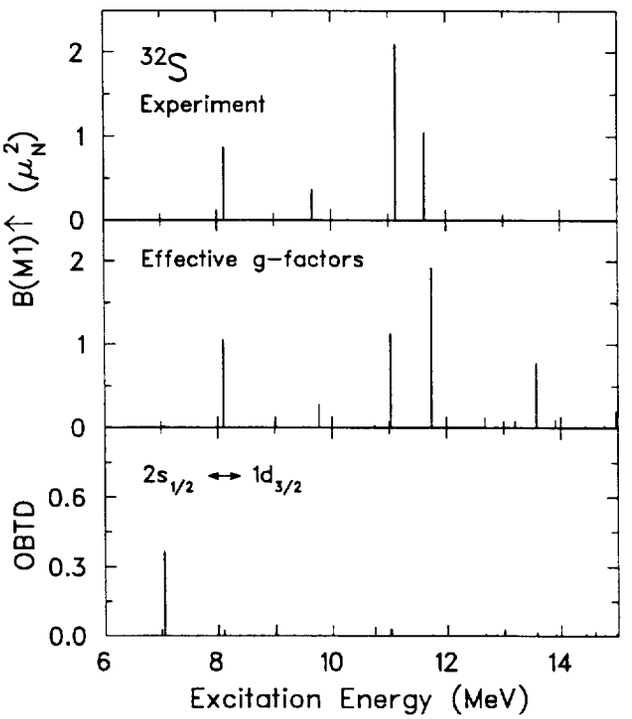

Figure 7: Comparison of the experimentally extracted M1 strength in ^{32}S with the prediction within the USD model by Brown and Wildenthal with effective g-factors. The one body transition density is highest for the ℓ-forbidden M1 transition to the $J^\pi = 1^+$ state at $E_x = 7.003$ MeV.

The reliability of the shell-model description was tested by comparison to the complete $B(\mathrm{M1})$ distribution in ^{32}S extracted from the experiments described above and the inclusion of previous data [46,47]. As visible in Fig. 7, a very good reproduction of the experimental strength distribution is achieved, even on a level-to-level basis. The only exception are the two prominent transitions between 11 and 12 MeV. However, their sharing of the g.s. $B(\mathrm{M1})$ strength is extremely sensitive to the energy difference and the total strength

is again described well. The lowest row of Fig. 7 displays the one-body transition density contributions of the ℓ-forbidden M1 transition to the $J^\pi = 1^+$ states. It confirms the dominant ℓ-forbidden character of the weak transition to the 7.003 MeV level.

In a more detailed analysis[48] it will be shown that shell-model calculations using empirical effective g-factors [42] permit a simultaneous description of the ℓ-forbidden and its analog GT transitions, if isospin mixing is taken into account [49]. On the other hand, such an agreement cannot be obtained with the correction factors predicted from the analytical calculations [43,44]. Thus, the present result on ^{32}S reinforce the problem encountered in the $A = 39$ nuclei which still seek a solution.

3.3 Second example: the magnetic quadrupole response in ^{48}Ca

A central goal of our work at the new 180° system are systematic investigations of the magnetic quadrupole response from light to heavy nuclei. Experimental information is rather scarce at present except for the lightest nuclei. The available data indicate a quenching which might be even more severe than for the M1 strength [38]. Besides the fundamental questions raised by such a result the amount of quenching and the M2 strength distributions of selected nuclei in the *sd*- and *fp*-shell are key ingredients for a detailed modeling of the late stages of heavy stars before a supernova collapse [50,51] and for the ν-nucleosynthesis process [52]. Furthermore, the spin part of the M2 strength is directly related to the $J^\pi = 2^-$ component of spin-dipole excitations [53] and might thus help to decompose the different angular momentum components.

We have chosen to study ^{48}Ca as a first example of a medium-mass nucleus for a number of reasons. The development of second-RPA (SRPA) theories [54] promises for the first time a realistic description of the properties of the M2 strength distributions in medium-mass and heavy nuclei. However, at present calculations can only be performed for closed-shell nuclei. A complementary ^{48}Ca($\vec{p}, \vec{p}$) experiment searching for the spin-dipole response is planned with the new focal-plane polarimeter at the KVI magnetic spectrometer within the EUROSUPERNOVA collaboration.

Figure 8 presents a typical ^{48}Ca(e,e') spectrum taken at 180°. Above 8 MeV the spectrum is dominated by transitions to 2^- states indicating a considerable fragmentation of the M2 strength. The spin information and reduced transition probabilities were derived from fits of RPA form factors to the experimental data. An example is shown in Fig. 9 for the prominent transition at 10.01 MeV, where data from previous measurements exist [55]. These are in good agreement with the new 180° results.

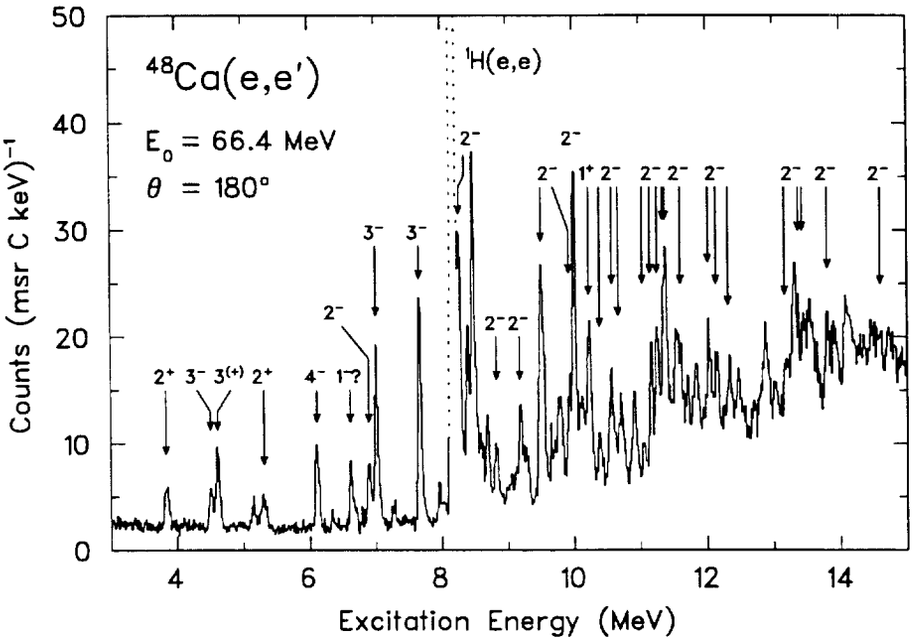

Figure 8: Inelastic electron scattering spectrum taken at $\theta = 180°$ and $E_0 = 66.4$ MeV in ^{48}Ca. The spins and parities of most states can be determined from form factor measurements at different momentum transfers q. The dotted line results from electrons elastically scattered off ^{1}H contaminating the ^{48}Ca target.

Similar to the example of dipole strength in heavy deformed odd-mass nuclei discussed in Sect. 2.3, the 2^- level density in ^{48}Ca above 11 MeV is so high that a fluctuation analysis must be applied to extract the complete B(M2) strength. The combined M2 strength distribution from the analysis of single transitions below 11 MeV and the fluctuation analysis in the region $11-15$ MeV is summarized in Fig. 10. It is compared to RPA and SRPA calculations using a M3Y interaction[56] and effective spin g-factors $g_s^{eff} = 0.75 g_s^{free}$ suggested by the systematics of GT strength in medium-heavy and heavy nuclei[57]. The RPA results predict a compact resonance at about 12 MeV in contrast to the strong fragmentation visible in the experimental results. However, if the coupling to $2p-2h$ excitations is taken into account in the SRPA calculation, the description is dramatically improved. Even details of the experimental strength distribution with clustering around 10, 12 and 15 MeV are reproduced within a few hundred keV. Also the resulting average strengths of single transitions

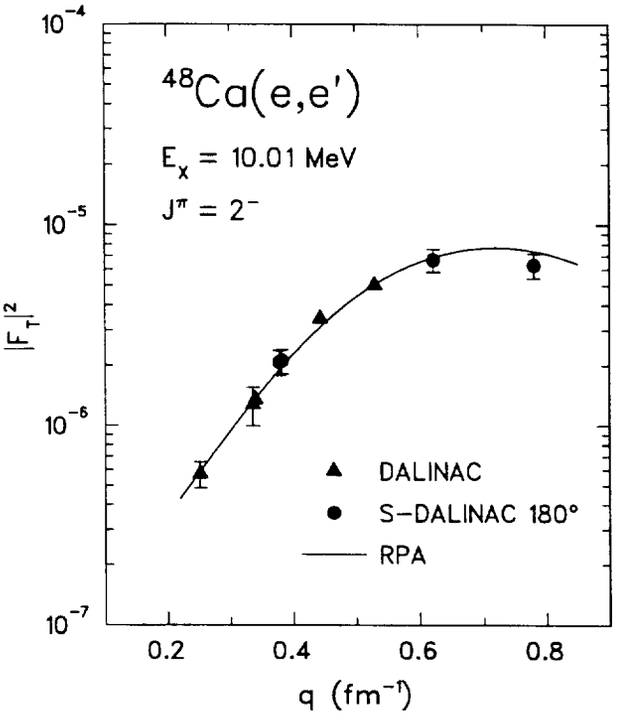

Figure 9: Form factor of the M2 transition to the $J^\pi = 2^-$ state at $E_x = 10.01$ MeV in ^{48}Ca measured in inelastic electron scattering at the DALINAC and the S-DALINAC. The curve represents the best fit of an RPA form factor prediction.

(or transitions into energy bins at higher E_x) are quite realistic. As already indicated by our first results with the 180° system in the lighter nucleus ^{28}Si the M2 giant resonance is spread out over a much larger energy interval than suggested by RPA calculations and this must be considered when comparing the data to sum rule predictions (see Sect. 3.6).

3.4 In-medium vector meson scaling and electron scattering form factors

The modification of nucleons and mesons by embedding them into the nuclear medium constitutes a central problem of nuclear physics which is experimentally addressed e.g. in high-energy heavy-ion reactions and electron scattering [58,59]. An important prediction has been made by Brown and Rho [60] that the effective masses should follow an approximate scaling corresponding to the

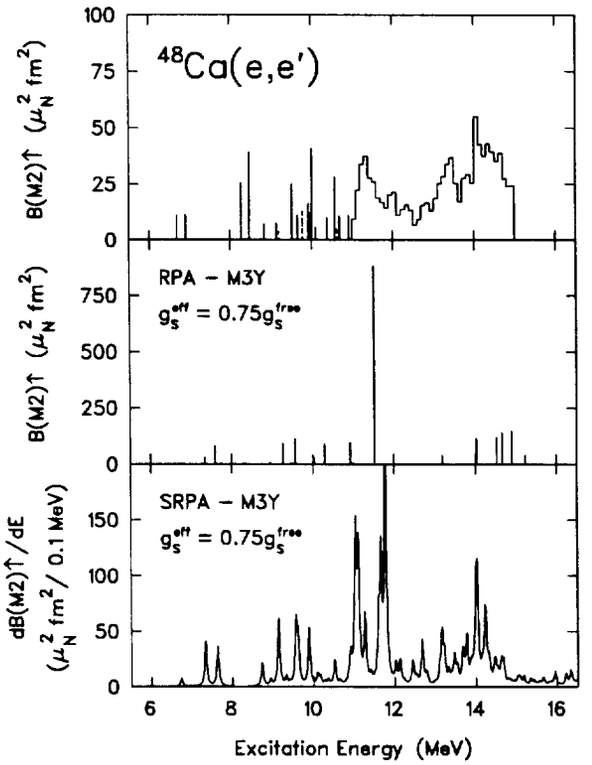

Figure 10: Comparison of the M2 strength distribution in ^{48}Ca with results of RPA and SRPA calculations. Since the RPA includes only $1p-1h$ excitations the fragmentation of the strength is not described sufficiently well. Only the consideration of $2p-2h$ excitations in the SRPA leads to a satisfactory agreement with the experimental results.

reduction of the pion coupling constant. This behaviour can be understood from a restauration of chiral symmetry at high baryon densities taking into account the scaling properties of QCD [61].

Although it seems at first sight remote, electron scattering at low energies and momentum transfers provides alternative access to this problem. As an example such effects have been investigated by Lallena [62] for transitions to low-lying unnatural parity states in ^{48}Ca using RPA and a modified form of the Jülich-Stony Brook interaction [63]. The calculations allow for a simultaneous variation of the ρ-meson mass and the pion coupling constant expressed by a parameter $\epsilon = (m_\rho/m_\rho^*)^2$, where m_ρ^* denotes the effective mass. Thus $\epsilon > 1$

leads to a simultaneous enhancement of the spin-isospin interaction and a reduction of the isovector tensor terms. The necessity of such modifications has been put forward by many authors (see e.g. Ref.[64] and references therein).

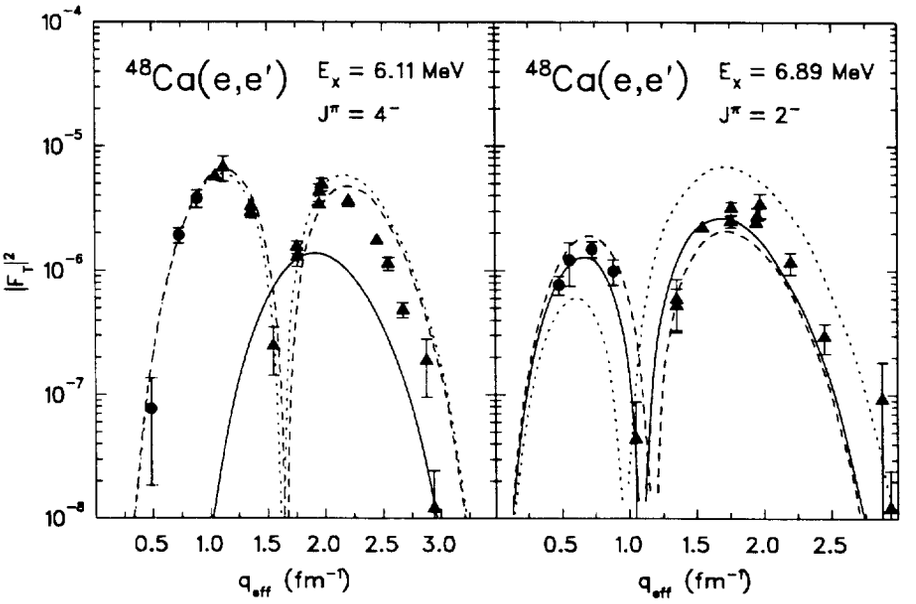

Figure 11: Form factors of the M4 and M2 transitions to the low lying $J^\pi = 4^-$ and $J^\pi = 2^-$ states at $E_x = 6.11$ MeV and 6.89 MeV in ^{48}Ca measured in inelastic electron scattering at the S-DALINAC and MIT-Bates. The curves represent calculations[62] for different values of the parameter ϵ.

Strong effects are visible in Fig. 11 for the M4 transition to the $E_x = 6.11$ MeV and the M2 transition to the $E_x = 6.89$ MeV levels due to variations of $\epsilon = 1$ (solid line), 1.2 (dashed line) and 1.6 (dotted line). These transitions have already been studied at MIT-Bates[65] for $q > 1$ fm^{-1} indicating the need for $\epsilon > 1$. The new data gained on ^{48}Ca by our 180° experiments described in the previous section clearly provide an upper constraint of $\epsilon \approx 1.2$ by the behaviour of the M2 transition around the first maximum of the form factor.

A word of caution is necessary, however, because the calcuations are based on rather severe approximations (e.g., no density dependence is included). Before one could draw quantitative conclusions on the effective ρ-meson mass, one should reinvestigate [66] the form factors with the very successful SRPA description discussed above (excluding any variations of meson masses) to get

some insight on the significance of the predictions of Ref. [62]. It should also be noted that a recent $(\vec{p},\vec{p}')$ experiment seems to question the need for any introduction of effective meson masses [67].

3.5 Third example: the magnetic quadrupole response in ^{90}Zr

With the experimental background improvements highlighted in Sect. 3.1 it has become possible to extend the 180° measurements to heavy nuclei also. As a first example, the semi-magic nucleus ^{90}Zr was studied. In previous high-resolution (e,e') experiments a compact M2 resonance was detected around 9 MeV, but the measurements were restricted to a limited energy interval [68,69]. The new findings on the M2 strength in ^{48}Ca raise the question whether significant parts of the M2 resonance are missed at higher excitation energies.

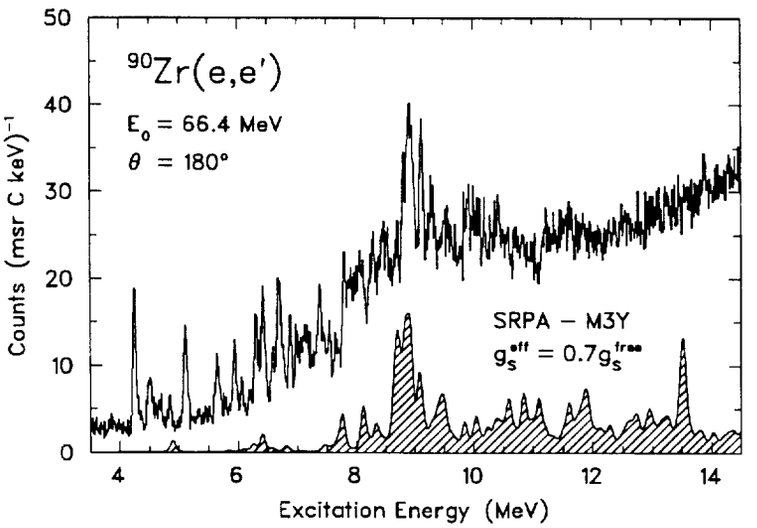

Figure 12: Inelastic electron scattering spectrum taken at $\theta = 180°$ and $E_0 = 66.4$ MeV in ^{90}Zr. For comparison the spectrum of M2 transitions calculated in SRPA is shown. The latter spectrum has been computed for the same kinematic conditions and folded with the experimental resolution.

Data in ^{90}Zr were taken up to energies of about 15 MeV. A typical spectrum obtained at $E_0 = 66.4$ MeV is plotted in Fig. 12. Below the spectrum the result of a SRPA calculation is shown as hatched area. The quenching is assumed to be the same as for the M1 strength and the resulting M2 distribution is folded with the experimental resolution and converted to cross sections

directly comparable to the data. The agreement with the prominent bump visible around 9 MeV, but also with structures around 11 and 12 MeV is remarkable. If one takes into account the radiative tail which already at low excitation energies (contrary to scattering at smaller angles) rises with E_x, the description is also satisfactory on a quantitative level.

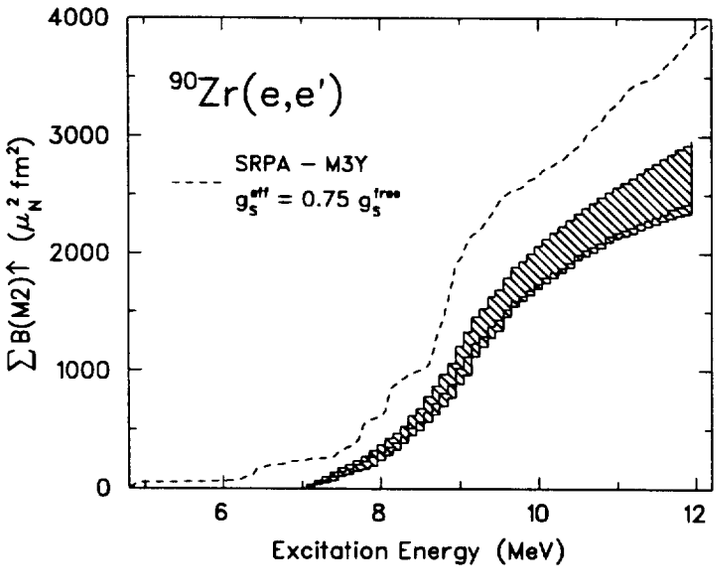

Figure 13: Cumulative sum of the M2 strength in ^{90}Zr exctracted with a statistical fluctuation analysis of the (e,e')-spectra taken at $\theta = 180°$ at the S-DALINAC. For comparison the result of an SRPA calculation with $g_s^{eff} = 0.75 g_s^{free}$ is shown.

In order to see to what extent the present results exhaust the theoretical M2 strength it is instructive to plot the running sum as a function of excitation energy (Fig. 13). The hatched area indicates the experimental uncertainty which is dominated by the assumptions about the level density in the fluctuation analysis. The B(M2) strength could be extracted up to $E_x \simeq 12$ MeV, at higher energies one probably enters the regime of Ericson fluctuations (i.e., overlapping levels) which precludes an application of the fluctuation analysis technique[31] used here. The dashed line represents the SRPA results assuming the effective spin g-factor as used for the ^{48}Ca results in Sect. 3.3. The rise with excitation energy is very satisfactorily accounted for, although a slightly larger quenching factor is suggested (see Sect. 3.6). However, there is no sign of saturation and an extension of the SRPA results up to 20 MeV indicates addi-

tional non-negligible contributions at higher energies which must be considered in the comparison to sum rules.

3.6 Sum rules for magnetic quadrupole strength

Finally, some remarks on the summed magnetic quadrupole strength in ^{48}Ca and ^{90}Zr are in order. In the respective excitation energy ranges $E_x = 4 - 15$ MeV and $E_x = 7 - 12$ MeV the observed non-energy weighted and energy weighted summed strengths are listed in Tab. 1.

Table 1: Non-energy weighted and energy weighted magnetic quadrupole strengths in ^{48}Ca and ^{90}Zr extracted in the experiment in the respective excitation energy ranges $E_x = 4 - 15$ MeV and $E_x = 7 - 12$ MeV.

		^{48}Ca	^{90}Zr
$\sum B(\mathrm{M2})\uparrow$	$(\mu_N^2 \mathrm{fm}^2)$	1260^{+300}_{-220}	2440^{+520}_{-110}
$\sum E_x B(\mathrm{M2})\uparrow$	$(\mu_N^2 \mathrm{fm}^2 \mathrm{MeV})$	15700^{+3400}_{-2400}	23800^{+3600}_{-1000}

Both the RPA and SRPA calculations with free g-factors overestimate the experimental strength substantially. Under the assumption that the M2 strength is almost entirely due to spin excitations – that this is indeed the case can be seen from an inspection of the SRPA amplitudes – an effective g-factor for the spin of $g_s^{eff} \approx 0.67 g_s^{free}$ can be derived by comparing the measured summed strengths with those calculated in the same excitation energy ranges. This quenching factor for M2 transitions is thus the same as observed in M1 and Gamow-Teller transitions.

The very good agreement between the experimentally determined fine structure and the one predicted by the SRPA calculations as discussed above in Sects. 3.3 and 3.5 allows furthermore an estimate of the M2 strength located still at excitation energies above the measured one. If the cumulative SRPA strength is normalized to the corresponding one from experiment the following non-energy weighted and energy weighted M2 strengths in ^{48}Ca and ^{90}Zr, respectively, are obtained: $\sum B(\mathrm{M2})\uparrow = 1780^{+420}_{-310}\ \mu_N^2 \mathrm{fm}^2$ and $4550^{+980}_{-270}\ \mu_N^2 \mathrm{fm}^2$, and $\sum E_x B(\mathrm{M2})\uparrow = 25000^{+5300}_{-3900}\ \mu_N^2 \mathrm{fm}^2 \mathrm{MeV}$ and $53100^{+7900}_{-2300}\ \mu_N^2 \mathrm{fm}^2 \mathrm{MeV}$. The respective model spaces in ^{48}Ca and ^{90}Zr in the SRPA calculations were thereby truncated at 70 MeV and 50 MeV for the $1p-1h$ states and at 27 MeV and 20 MeV for the $2p-2h$ states.

Those "quasi-experimental" summed strengths can be compared to sum rules. Firstly, a comparison with a non-energy weighted sum rule (NEWSR)

by Kurath [70] within an oscillator shell model shows that the data exhaust only about one third of the predicted strength. Hence an effective g-factor $g_s^{eff} \approx 0.58 g_s^{free}$ is obtained which is not too different from the one derived independently from a comparison of the data with the SRPA prediction. Secondly, an energy weighted sum rule (EWSR) for spin-isospin magnetic multipole strength exists which Traini [71] has found through a generalization of Kurath's sum rule for magnetic dipole transitions in self-conjugate nuclei [72]. Figure 14 (which is an update of a similar figure in Ref. [38]) summarizes the resulting EWSR predictions compared to the world's data on M2 strengths. Except

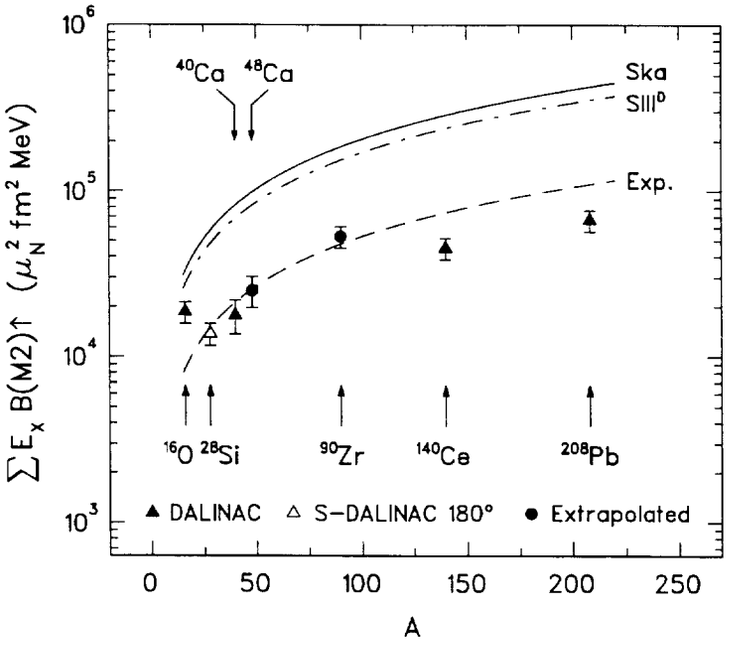

Figure 14: Energy weighted sum rule values of all available M2 strength distributions as a function of mass number. The dashed line is an empirical fit to the data. The dashed-dotted and solid lines represent EWSR predictions [71] using two different effective Skyrme forces.

for the lightest nuclei, all experimental results are from Darmstadt [38,68,73,74]. A common trend is observed. With respect to the model predictions (with two different Skyrme forces [71]) a strong suppression of M2 strength is found. For ^{48}Ca and ^{90}Zr the measured and extrapolated EWSR strengths again (as it was the case for the NEWSR strength) exhaust only about one third of the sum rule prediction, which again results in a quenching factor of 0.58 for the

spin g-factor. It should also be noted that from what we have learned from the present experiments on ^{48}Ca and ^{90}Zr the two points for ^{140}Ce and ^{208}Pb in Fig. 14 are below the extrapolated line since most likely not all M2 strength has been detected in the latter experiments. A further comparison of our data with a sum rule for spin-dependent excitations derived by Suzuki [75] model independently is presently underway.

4 Conclusions and outlook

In the first part of the talk I have discussed some salient features of the orbital and spin magnetic dipole response which still is not fully understood. The *weakly* collective orbital strength, which is – qualitatively speaking – made up from small angle vibrations of neutrons vs. protons in a scissors-like motion, shows a dependence upon the quadrupole deformation of the nuclear ground state and hence points to a particular feature of the quadrupole-quadrupole force driving the nucleus to deformation. From sum rule considerations we can argue that experimentally all orbital M1 strength is found in heavy deformed nuclei. The spin strength – as is demonstrated beautifully by the example in Fig. 1 – is removed from the orbital strength by the repulsive spin-isospin force up to higher excitation energy. It is independent of deformation, *strongly* collective and shows the phenomenon of quenching, which is still with us since about two decades and basically unexplained theoretically.

In the second part of the talk I have first explained the powerful 180°-scattering facility at the S-DALINAC for the study of magnetic transitions and then discussed mainly the magnetic quadrupole response in ^{48}Ca and ^{90}Zr, i.e. the $J^\pi = 2^-$ part of the so called spin-dipole resonance consisting of $J^\pi = 0^-, 1^-$ and 2^- pieces[53,76]. As has been pointed out by a comparison with SRPA as well as with NEWSR and EWSR predictions the magnetic quadrupole strength is quenched by the same amount as the magnetic dipole strength. In future experiments we will extend our measurements to still higher excitation energies in order to pick up possible remaining M2 strength as well as (for the first time) the transverse E1 strength into the $J^\pi = 1^-$ member of the spin-dipole resonance which is expected to lie several MeV above the center of the M2 strength [77,78].

As has been emphazised in Ref. [38] the experimentally precisely determined low-energy nuclear structure information on the magnetic dipole and quadrupole response may also give insight into astrophysical problems like the dynamics of stellar collapse and nucleosynthesis during the shock wave of a supernova. I have had no time to discuss this topic here but should finally remark, that the future experimental program at the 180° system at the S-DALINAC forms part

of an international effort by the so called EUROSUPERNOVA collaboration including research groups from U Bari, TU Darmstadt, U Gent, KVI Groningen, U Madrid, U Milano and U Münster which aims at an experimental determination of magnetic properties of nuclei relevant to astrophysical problems by combining high-resolution medium energy polarized proton scattering at small angles with 180° electron scattering.

Acknowledgments

I am very much indebted to my many collaborators at the S-DALINAC and elsewhere. I mention in particular B.A. Brown, J. Enders, D. Frekers, J.N. Ginocchio, H.-D. Gräf, K. Heyde, F. Hofmann, the late N. Huxel, H. Kaiser, U. Kneissl, N. Lo Iudice, P. von Neumann-Cosel, F. Neumeyer, C. Rangacharyulu, B. Reitz, G. Schrieder, D.I. Sober and I.S. Towner for sharing their insight with me into the various topics discussed here. Many thanks go also to J. Wambach and his collaborators A. May, S. Nishizaki, V. Ponomarev and T. Waindzoch for performing the SRPA calculations in ^{48}Ca and ^{90}Zr and for many discussions. Finally, P. von Neumann-Cosel and F. Neumeyer have not only contributed greatly to the physics which I presented but also helped me in preparing the manuscript of the talk. At the same time I am grateful to Hide Sakai for having provided a very stimulating atmosphere at SGR97 in Tokyo. This work has been supported by the Deutsche Forschungsgemeinschaft under contract Ri242/12-1.

References

1. A. Richter in *Proc. 5th EPAC*, ed. S. Myers *et al.* (IOP Publishing, Bristol, 1996).
2. A. Richter, *Nucl. Phys.* A **522**, 139c (1991).
3. A. Richter, *Prog. Part. Nucl. Phys.* **34**, 261 (1995).
4. M. Macfarlane, J. Speth and D. Zawischa, *Nucl. Phys.* A **606**, 41 (1996).
5. A. Faessler, *Prog. Part. Nucl. Phys.* **38**, 195 (1997).
6. D. Bohle, A. Richter, W. Steffen, A.E.L. Dieperink, N. Lo Iudice, F. Palumbo and O. Scholten, *Phys. Lett.* B **137**, 27 (1984).
7. D. Frekers, D. Bohle, A. Richter, R. Abegg, R.F. Azuma, A. Celler, C. Chan, T.E. Drake, K.P. Jackson, J.D. King, C.A. Miller, R. Schubank, J. Watson and S. Yen, *Phys. Lett.* B **218**, 439 (1989).
8. D. Frekers, H.J. Wörtche, A. Richter, R. Abegg, R.E. Azuma, A. Celler, C. Chan, T.E. Drake, R. Helmer, K.P. Jackson, J.D. King, C.A. Miller, R. Schubank, M.C. Vetterli and S. Yen, *Phys. Lett.* B **244**, 178 (1990).

9. W. Ziegler, C. Rangacharyulu, A. Richter and C. Spieler, *Phys. Rev. Lett.* **65**, 2515 (1990).
10. C. Rangacharyulu, A. Richter, H.J. Wörtche, W. Ziegler and R.F. Casten, *Phys. Rev.* C **43**, R949 (1991).
11. C. Djajali, N. Marty, M. Morlet, A. Willis, J.C. Jourdain, D. Bohle, U. Hartmann, G. Küchler, A. Richter, G. Caskey, G.M. Crawley and A. Galonsky, *Phys. Lett.* B **164**, 269 (1985).
12. P. von Neumann-Cosel, *Prog. Part. Nucl. Phys.* **38**, 213 (1997).
13. U. Kneissl, H.H. Pitz and A. Zilges, *Prog. Part. Nucl. Phys.* **37**, 439 (1996).
14. E. Lipparini and S. Stringari, *Phys. Lett.* B **130**, 139 (1983).
15. N. Lo Iudice and A. Richter, *Phys. Lett.* B **304**, 193 (1993).
16. N. Lo Iudice and F. Palumbo, *Phys. Rev. Lett.* **41**, 1532 (1978).
17. A. Bohr and B.R. Mottelson, *Nuclear Structure - Vol. II* (W.A. Benjamin, New York-Amsterdam, 1975).
18. P. von Neumann-Cosel, J.N. Ginocchio, H. Bauer and A. Richter, *Phys. Rev. Lett.* **75**, 4178 (1995).
19. J.N. Ginocchio, *Phys. Lett.* B **265**, 6 (1991).
20. P. von Brentano, J. Eberth, J. Enders, L. Esser, R.-D. Herzberg, N. Huxel, H. Meise, P. von Neumann-Cosel, N. Nicolay, N. Pietralla, H. Prade, J. Reif, A. Richter, C. Schlegel, R. Schwengner, S. Skoda, H.G. Thomas, I. Wiedenhöver, G. Winter and A. Zilges, *Phys. Rev. Lett.* **76**, 2029 (1996).
21. H. Maser, N. Pietralla, P. von Brentano, R.-D. Herzberg, U. Kneissl, J. Margraf, H.H. Pitz and A. Zilges, *Phys. Rev.* C **54**, R2129 (1996).
22. A. Zilges, P. von Brentano, H. Friedrichs, R.D. Heil, U. Kneissl, S. Lindenstruth, H.H. Pitz and C. Wesselborg, *Z. Phys.* A **340**, 155 (1991).
23. I. Bauske, J.M. Arias, P. von Brentano, A. Frank, H. Friedrichs, R.D. Heil, R.-D. Herzberg, F. Hoyler, P. van Isacker, U. Kneissl, J. Margraf, H.H. Pitz, C. Wesselborg and A. Zilges, *Phys. Rev. Lett.* **71**, 975 (1993).
24. J. Margraf, T. Eckert, M. Rittner, I. Bauske, H. Maser, H.H. Pitz, A. Schiller, P. von Brentano, R. Fischer, R.-D. Herzberg, N. Pietralla, A. Zilges and H. Friedrichs, *Phys. Rev.* C **52**, 2429 (1995).
25. C. Schlegel, P. von Neumann-Cosel, A. Richter and P. Van Isacker, *Phys. Lett.* B **375**, 21 (1996).
26. A. Nord, A. Schiller, T. Eckert, O. Beck, J. Besserer, P. von Brentano, R. Fischer, R.-D. Herzberg, D. Jäger, U. Kneissl, J. Margraf, H. Maser, N. Pietralla, H.H. Pitz, M. Rittner and A. Zilges, *Phys. Rev.* C **54**, 2287 (1996).

27. N. Huxel, Doctoral Thesis, D17, TU Darmstadt (1997); and to be published.
28. V.G. Soloviev, A.V. Shuskov and N.Yu. Shirikova, *Phys. Rev.* C **53**, 1022 (1996);
V.G. Soloviev, A.V. Shuskov, N.Yu. Shirikova and N. Lo Iudice, *Nucl. Phys.* A **613**, 47 (1997).
29. J.N. Ginocchio and A. Leviatan, *Phys. Rev. Lett.* **79**, 813 (1997).
30. J. Enders, N. Huxel, P. von Neumann-Cosel and A. Richter, *Phys. Rev. Lett.* **79**, 2010 (1997).
31. P.G. Hansen, B. Jonson and A. Richter, *Nucl. Phys.* A **518**, 13 (1990).
32. J. Enders, N. Huxel, U. Kneissl, P. von Neumann-Cosel, H.H. Pitz and A. Richter, *Phys. Rev.* C, in press.
33. C. Lüttge, C. Hofmann, J. Horn, F. Neumeyer, A. Richter, G. Schrieder, E. Spamer, A. Stiller, D.I. Sober, S.K. Matthews and L.W. Fagg, *Nucl. Instrum. Methods* A **366**, 325 (1995).
34. H. Diesener, U. Helm, G. Herbert, V. Huck, P. von Neumann–Cosel, C. Rangacharyulu, A. Richter, G. Schrieder, A. Stascheck, A. Stiller, J. Ryckebusch and J. Carter, *Phys. Rev. Lett.* **72**, 1994 (1994).
35. F. Neumeyer, Doctoral Thesis, D17, TU Darmstadt (1997); and to be published.
36. S. Döbert, R. Eichhorn, H. Genz, H.-D. Gräf, R. Hahn, H. Loos, A. Richter, B. Schweizer, A. Stascheck and T. Wesp, *Phys. Rev.* E, submitted.
37. C. Lüttge, P. von Neumann-Cosel, F. Neumeyer, C. Rangacharyulu, A. Richter, G. Schrieder, E. Spamer, D.I. Sober, S.K. Matthews and B.A. Brown, *Phys. Rev.* C **53**, 127 (1996).
38. C. Lüttge, P. von Neumann-Cosel, F. Neumeyer and A. Richter, *Nucl. Phys.* A **606**, 183 (1996).
39. P. von Neumann-Cosel, A. Richter, Y. Fujita and B.D. Anderson, *Phys. Rev.* C **55**, 532 (1997).
40. A. Richter, A. Weiss, O. Häusser and B.A. Brown, *Phys. Rev. Lett.* **65**, 2519 (1990).
41. B.A. Brown and B.H. Wildenthal, *Annu. Rev. Nucl. Part. Sci.* **38**, 29 (1988).
42. B.A. Brown and B.H. Wildenthal, *Nucl. Phys.* A **474**, 290 (1987).
43. I.S. Towner and F.C. Khanna, *Nucl. Phys.* A **399**, 334 (1983).
44. A. Arima, K. Shimizu, W. Bentz and H. Hyuga, *Adv. Nucl. Phys.* **18**, 1 (1987).
45. E. Hagberg, T.K. Alexander, I. Neeson, V.T. Koslowsky, G.C. Ball, G.R. Dyck, J.S. Foster, J.C. Hardy, J.R. Leslie, H.-B. Mak, H. Schmeing

and I.S. Towner, *Nucl. Phys.* A **571**, 555 (1994).
46. M. Petraitis, J.P. Connely, H. Crannell, L.W. Fagg, J.T. O'Brien, D.I. Sober, J.R. Deininger, S.E. Williamson, R. Lindgren and S. Raman, *Phys. Rev.* C **49**, 3000 (1994).
47. P.E. Burt, L.W. Fagg, H. Crannell, D.I. Sober, W. Stapor, J.T. O'Brien, J.W. Lightbody, X.K. Maruyama, R.A. Lindgren and C.P. Sargent, *Phys. Rev.* C **29**, 713 (1984).
48. B. Reitz, P. von Neumann-Cosel, F. Neumeyer, C. Rangacharyulu, A. Richter, G. Schrieder, D.I. Sober and B.A. Brown, to be published.
49. W.E. Ormand and B.A. Brown, *Nucl. Phys.* A **491**, 1 (1989).
50. A. Zaringhalam, *Nucl. Phys.* A **404**, 599 (1983).
51. J. Cooperstein and J. Wambach, *Nucl. Phys.* A **420**, 591 (1984).
52. S.E. Woosley, D.H. Hartmann, R.D. Hofmann and W.C. Haxton, *Astrophys. J.* **356**, 272 (1990).
53. F. Osterfeld, *Rev. Mod. Phys.* **64**, 491 (1992).
54. S. Drożdż, S. Nishizaki, J. Speth and J. Wambach, *Phys. Rep.* **197**, 1 (1990).
55. W. Steffen, Doctoral Thesis, D17, TU Darmstadt (1984).
56. G.F. Bertsch, J. Borysowicz, H. McManus and W.G. Love, *Nucl. Phys.* A **284**, 399 (1977).
57. C. Gaarde in *Proc. of the Niels Bohr Cent. Conf. on Nuclear Structure*, ed. R. Broglia *et al.* (North-Holland, Amsterdam, 1985).
58. *Proc. 12th Int. Conf. on Ultra-Relativistic Nucleus-Nucleus Collisions*, eds. P. Braun-Munzinger, H.J. Specht, R. Stock and H. Stöcker, *Nucl. Phys.* A **610**, 1c (1996).
59. M. Soyeur, G.E. Brown and M. Rho, *Nucl. Phys.* A **556**, 355 (1993).
60. G.E. Brown and M. Rho, *Phys. Rev. Lett.* **66**, 2720 (1991).
61. F. Klingl, N. Kaiser, W. Weise, *Nucl. Phys.* A **624**, 527 (1997).
62. A.M. Lallena, *Phys. Rev.* C **48**, 344 (1993).
63. J. Speth, V. Klemt, J. Wambach and G.E. Brown, *Nucl. Phys.* A **343**, 382 (1980).
64. M.S. Fayache, P. von Neumann-Cosel, A. Richter, Y.Y. Sharon and L. Zamick, *Nucl. Phys.* A **627**, 14 (1997).
65. J.E. Wise, J.S. McCarthy, R. Altemus, B.E. Norum, R.R. Whitney, J. Heisenberg, J. Dawson and O. Schwentker, *Phys. Rev.* C **31**, 1699 (1985).
66. J. Wambach, private communication.
67. E.J. Stephenson, J. Liu, A.D. Bacher, S.M. Bowyer, S. Chang, C. Olmer, S.P. Wells, S.W. Wissink and J. Lisantti, *Phys. Rev. Lett.* **78**, 1636 (1997).

68. D. Meuer, R. Frey, D.H.H. Hofmann, A. Richter, E. Spamer, O. Titze and W. Knüpfer, *Nucl. Phys.* A **349**, 309 (1980).
69. S. Müller, F. Beck, D. Meuer and A. Richter, *Phys. Lett.* B **113**, 362 (1982).
70. D. Kurath, Report *ANL* **97/14**, 161 (1997); and private communication.
71. M. Traini, *Phys. Rev. Lett.* **41**, 1535 (1978).
72. D. Kurath, *Phys. Rev.* **130**, 1525 (1963).
73. W. Knüpfer, R. Frey, A. Friebel, W. Mettner, D. Meuer, A. Richter, E. Spamer and O. Titze, *Phys. Lett.* B **77**, 367 (1978).
74. D. Meuer, G. Kühner, S. Müller, A. Richter, E. Spamer, O. Titze and W. Knüpfer, *Phys. Lett.* B **106**, 289 (1981).
75. T. Suzuki, *Ann. Phys. Fr.* **9**, 535 (1984).
76. F.T. Baker, L. Bimbot, C. Djalali, C. Glashausser, H. Lenske, W.G. Love, M. Morlet, E. Tomasi-Gustafsson, J. van de Wiele, J. Wambach and A. Willis, *Phys. Rep.* **289**, 1 (1997).
77. C. Gaarde, J. Rapaport, T.N. Taddeucci, C.D. Goodman, C.C. Foster, D.E. Bainum, C.A. Goulding, M.B. Greenfield, D.J. Horen and E. Sugarbaker, *Nucl. Phys.* A **369**, 258 (1981).
78. V.Yu. Ponomarev, A.I. Vdovin, V.M. Shilov and Nguyen Dinh Dang, *Phys. Scrip.* **30**, 238 (1984).